Acta Crystallographica Section B
Structural Science
ISSN 0108-7681

Incommensurately modulated phase of Rb_2CoBr_4 at 295 and 200 K

K. Friese,[a]* G. Madariaga[a] and T. Breczewski[b]

[a]Departamento de Física de la Materia Condensada, Universidad del País Vasco, Apdo. 644, 48080 Bilbao, Spain, and [b]Departamento de Física Aplicada II, Universidad del País Vasco, Apdo. 644, 48080 Bilbao, Spain

Correspondence e-mail: wmbfrxxk@lg.ehu.es

Received 1 April 1999
Accepted 5 August 1999

The crystal structure of Rb_2CoBr_4 at 295 and 200 K has been determined. At these temperatures Rb_2CoBr_4 exhibits an incommensurately modulated structure with wavevector $\mathbf{q} = (1/3 + \delta)\mathbf{a}^*$. At room temperature only the average structure was refined. Lattice parameters are a = 9.732 (3), b = 13.328 (4), c = 7.654 (3) Å, space group *Pnam*. The $R(F)$ value was 0.0414 for 286 observed reflections (0.0778 for all 477 reflections). At 200 K the lattice parameters are a = 9.691 (4), b = 13.278 (5), c = 7.630 (6) Å, superspace group $P{:}Pnam{:}\bar{1}ss$. Main reflections and satellite reflections of first order were measured. The refinement converged at $R(F)$ = 0.052 for 309 observed reflections (255 main reflections and 54 satellites) and 0.2971 for all reflections (1849; 695 main reflections and 1154 satellites). Amplitudes and phases of the modulation function as well as bond distances show close relationships to those observed in the incommensurately modulated phase of Rb_2ZnBr_4.

1. Introduction

Rb_2CoBr_4, dirubidium cobalt tetrebromide, belongs to the family of A_2BX_4 compounds which at high temperature are isomorphous to β-K_2SO_4. Dielectric measurements suggest four possible phase transitions at approximately 333, 192, 98 and 65 K (Gesi, 1985; Yamaguchi *et al.*, 1987).

Above 333 K the structure is isomorphous to β-K_2SO_4 with space group *Pnam* (Seifert & Al-Khudair, 1975). Lattice parameters for this phase at 348 K were given as a = 9.724 (3), b = 13.337 (4) and c = 7.643 (2) Å (Kasano *et al.*, 1987). The first phase transition at 333 K leads to an incommensurately modulated structure with a $\mathbf{q}$ vector of $(0.3333 \pm \delta)\mathbf{a}^*$. X-ray studies near T_i show δ to be around 0.032 (Kasano *et al.*, 1987). This incommensurate phase locks-in to a ferroelectric phase at a temperature of 193 K, which, analogous to Rb_2ZnBr_4, is supposed to posses a wavevector of $1/3\mathbf{a}^*$ (Sawada *et al.*, 1978). Furthermore, the dielectric measurements indicate two more phase transitions which correspond to the temperatures of 95 (98) and 65 K (Gesi, 1985; Yamaguchi *et al.*, 1987).

For the family of A_2BX_4 compounds stereochemical criteria have been established to predict the occurrence of phase transitions at lower temperatures (see *e.g.* Fábry & Pérez-Mato, 1994), yet there is still need for more structural data to be sure about their reliability. As no structural data are known so far for the proposed phases of Rb_2CoBr_4, we thought it worthwhile to carry out X-ray structural investigations to gain more insight into the empirical parameters

Table 1
Experimental conditions and structure refinement.

	293 K	200 K
(Super) space group	*Pnam*	*P*:*Pnam*:$\bar{1}ss$
a (Å)	9.732 (3)	9.691 (4)
b (Å)	13.328 (4)	13.278 (5)
c (Å)	7.654 (3)	7.630 (6)
Lattice parameters from	1204 reflections	707 reflections
V (Å^3)	992.8 (6)	981.8 (2)
μ (mm^{-1})	27.48	27.48
Diffractometer	Stoe IPDS	Stoe IPDS
Wavelength (Å)	0.71073	0.71073
Phi-range (°)	0–200	0–228
Phi increment (°)	2	2
Exposure time (min)	10	30
Distance IPDS (mm)	110	90
2θ range	2.1–39.3	2.5–45.0
hkl_{min}–hkl_{max}	$\bar{9}$,$\bar{1}\bar{2}$,$\bar{7}$–9,11,7	$\bar{1}\bar{0}$, $\bar{1}\bar{4}$, $\bar{8}$, $\bar{1}$–10,13,8,1
Profile function	θ-dependent	θ-dependent
Minimum profile diameter (pixel)	11	11
Maximum profile diameter (pixel)	17	17
Effective mosaic spread	0.015	0.015
Approximate crystal size (mm)	0.1 × 0.1 × 0.06	0.1 × 0.1 × 0.06
Crystal shape	Irregular	Irregular
Approximated by	14 faces	14 faces
Absorption correction	Gauss	Gauss
T_{min}, T_{max}	0.0239, 0.0755	0.0239, 0.0755
With program	*XRED* (Stoe & Cie, 1998*b*)	*XRED* (Stoe & Cie, 1998*b*)
Unique reflections	477	1849 (695 main + 1154 satellite)
Reflections $\geq 4\sigma$	286	309 (255 main + 54 satellite)
$R(F^2)_{int}$	0.123	0.166
Structure refinement	*SHELXL*93 (Sheldrick, 1993)	*JANA*98 (Petříček & Dušek, 1998)
R (observed)	0.0414 (*FO* $\geq 4\sigma$)	0.0515 (*FO* $\geq 3\sigma$) (m = 0: 0.0477/$m \neq$ 0: 0.0838)
R (all)	0.0778 (*FO*)	0.2971 (*FO*) (m = 0: 0.1584/$m \neq$ 0: 0.5557)
wR(all)	0.1003 (*FO*^{2})	0.0494 (*FO*) (m = 0: 0.0399/$m \neq$ 0: 0.2518)
Weighting scheme	$w = 1/[\sigma^2(F_{obs})^2 + (0.0518P)^2]$, where $P = (\mathrm{Max}(F_{obs})^2 + 2(F_{calc})^2)/3$	$1/\sigma(F_{obs})^2$
Extinction correction	None	None

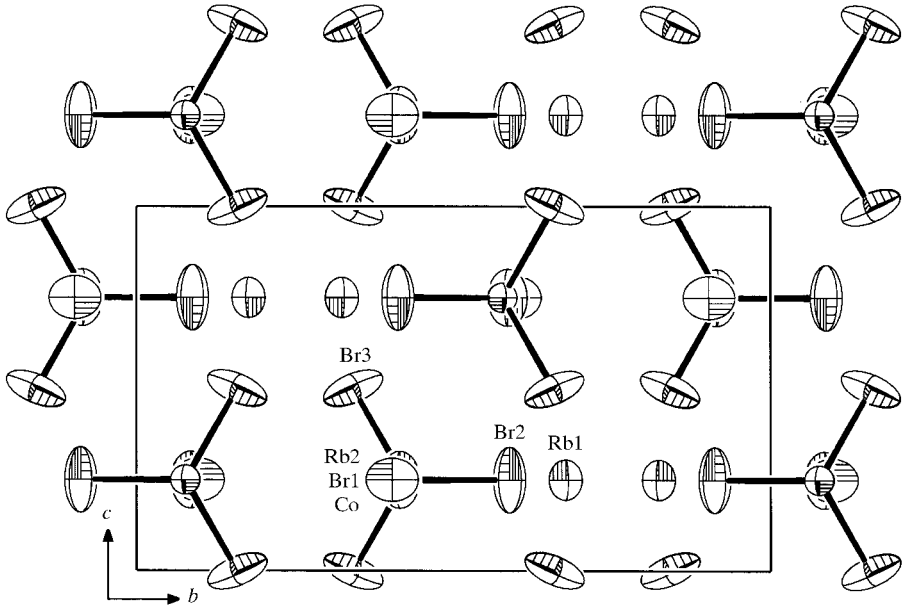

Figure 1
bc projection of the average structure of Rb_2CoBr_4 at 295 K; drawn with *ORTEP*3 (Farrugia, 1996).

influencing the structural stability in this large family of compounds.

2. Experimental

Single crystals were grown by fusion. For this a mixture of RbBr and $CoBr_2$ (well dried) was sealed within a silica crucible *in vacuo* in the stochiometric molar ratio. The mixture was heated up to 520 K, kept at this temperature for 24 h and afterwards slowly cooled down to 400 K with a rate of 1 K h^{-1}. Further cooling to 295 K was carried out with a rate of 5 K h^{-1}.

The obtained crystals were of greenish-blue colour and irregular shape. They were generally of poor quality and highly hygroscopic. For diffraction experiments it was necessary to enclose them in a capillary, embedding them in oil. Without this they decomposed rapidly (within approximately 20 min in air), changing their colour from greenish-blue to pink. The resulting product was amorphous.

Data collection was carried out using a Stoe IPDS diffractometer at room temperature and 200 K. For cooling the Oxford Cryostream system was used. All the investigated crystals diffract very poorly and generally above $\theta = 20°$ we could not observe any intensity. At room temperature we thus chose a distance of 110 mm from the sample for the imaging plate (corresponding to a θ_{max} of 20°). At the lower temperature diffracted intensity was observed at slightly higher θ angles and we used a distance of 90 mm ($\theta_{max} = 22.5°$).

Owing to their very weak intensity we were not able to measure the satellite reflections at room temperature, yet lowering the temperature to 200 K we could observe a small number of first-order satellites. Refinement of the wavevector (Stoe & Cie, 1998*a*) led to a value of $\mathbf{q}$ = (0.31,0,0). Extinction rules indicated the space group *Pnam* for the average structure at room temperature and the superspace group *P*:*Pnam*:$\bar{1}ss$ at 200 K.

Table 2
Positional and equivalent thermal displacement parameters (in Å^2) for Rb_2CoBr_4.

First line: coordinates of atoms in the average structure at room temperature; second line: basic coordinates of the atoms at 200 K.

	x	*y*	*z*	U_{eq}
Rb1	0.0149 (3)	0.6764 (2)	0.25	0.0570 (9)
	0.0132 (4)	0.6755 (3)	0.25	0.038 (2)
Rb2	0.3712 (3)	0.4028 (3)	0.25	0.087 (1)
	0.3736 (4)	0.4025 (4)	0.25	0.063 (2)
Co	0.7742 (4)	0.4231 (3)	0.25	0.039 (1)
	0.7760 (4)	0.4232 (4)	0.25	0.035 (2)
Br1	0.0183 (3)	0.4149 (3)	0.25	0.087 (1)
	0.0196 (4)	0.4160 (4)	0.25	0.056 (3)
Br2	0.6802 (4)	0.5881 (3)	0.25	0.101 (2)
	0.6771 (4)	0.5864 (4)	0.25	0.050 (3)
Br3	0.6840 (3)	0.3414 (2)	0.5013 (3)	0.102 (1)
	0.6869 (4)	0.3395 (3)	0.5003 (6)	0.062 (2)

Lattice parameters and further details concerning the experimental conditions are given in Table 1.[1]

3. Structure determination

Refinement was carried out with the programs *SHELXL* (Sheldrick, 1993) and *JANA*98 (Petříček & Dušek, 1998) using the coordinates of Cs_2ZnI_4 (Friese *et al.*, 1998) as a starting model for the average structures. Details concerning the refinement are given in Table 1; final atomic coordinates, displacement parameters and Fourier coefficients of the modulation functions are given in Tables 2 and 3.

4. Comparison to related compounds and discussion

The average structure of Rb_2CoBr_4 at room temperature is isomorphous to β-K_2SO_4 and, like this, is pseudohexagonal, with **a** as the pseudohexagonal axis. Within the structure two types of *A* cations can be observed, one has coordination 9 (Rb1) with bond distances ranging from 3.465 (6) to 4.029 (2) Å, while the other has coordination 11 (Rb2) with distances between 3.436 (5) and 4.470 (5) Å (see Table 4). The Co atom is surrounded tetrahedrally by Br with bond distances between 2.378 (4) and 2.381 (6) Å (see Fig. 1). Bond valence sums lead to values of 1.081, 0.628 and 2.335 v.u. (valence units) for Rb1, Rb2 and Co, respectively. The displacement parameters of the atoms are extremely high in some directions (see Fig. 1), indicating the structural modulation.

In the incommensurate phase at 200 K **a** represents the direction of the modulation wavevector. The highest modulation amplitudes are observed for Br1 and Br2 along the *z* direction, as well as along the *y* direction for Br3; smallest modulation amplitudes are observed for Co.

To analyze the structural modulation of Cs_2ZnI_4 and to compare it with the patterns observed in other A_2BX_4 compounds a symmetry mode analysis was carried out (for symmetry mode analysis see *e.g.* Pérez-Mato *et al.*, 1986; Pérez-Mato *et al.*, 1989; Friese *et al.*, 1999). The Σ_2 mode can be considered the primary mode which restricts the distortion symmetry at a maximum. The atomic displacements corresponding to this primary distortion are restricted along the **z** axis for the atoms which lie on the mirror plane in the *Pnam* phase and only the atom Br3 has Σ_2 displacements along the **x** and **y** directions. Comparison of the amplitudes and phases of the Σ_2 mode of Rb_2CoBr_4 with those observed in other A_2BX_4 compounds show an extremely good agreement with Rb_2ZnBr_4 (see Fig. 2). The same type of correspondence was already observed between the lock-in phase of Cs_2ZnI_4 and Cs_2CdBr_4 and it seems as if it is the *A* cation which mainly determines the amplitudes and phases of this mode (Friese *et al.*, 1999).

Bond lengths and bond valence sums as a function of the intrinsic parameter *t* are given in Figs. 3 and 5. Variation of distances in the $[CoBr_4]^{2-}$ tetrahedra is comparatively small. While Co—Br1 distances are nearly constant (2.363–2.375 Å), Co—Br2 distances show a greater variation (2.370–2.406 Å) and Co—Br3 distances exceed over a considerable range (2.346–2.445 Å; Table 4).

Rb—Br bond distances exceed over a large range. The largest variation of ~1 Å in bond lengths are observed for Rb2—Br3^{ii,iii} and Rb2—Br3^{x,xi}. These are followed by the bond lengths Rb1—Br1^{vii,vii} (0.85 Å) and Rb2—Br2^{ii,vii} (0.76 Å). A large group of bond lengths are almost constant or show only small variations (≥ 0.1 Å; Fig. 3, Table 4).

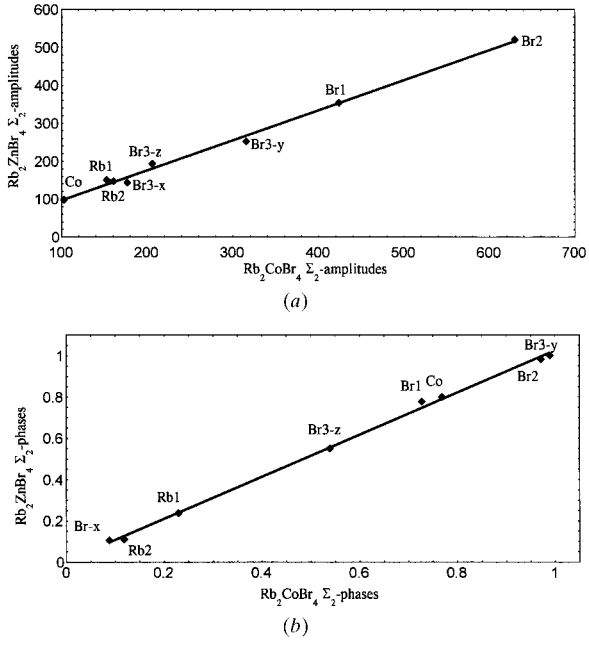

Figure 2
Comparison of the Σ_2 primary mode in Rb_2CoBr_4 and Rb_2ZnBr_4: (*a*) amplitudes (relative coordinates in units of 10^{-2}) and (*b*) phases (in units of 2π).

[1] Supplementary data for this paper are available from the IUCr electronic archives (Reference: SH0133). Services for accessing these data are described at the back of the journal.

Table 3
Fourier coefficient of the modulation function of Rb_2CoBr_4 at 200 K.

The modulation function is defined as $U_1^{\mu}(\bar{x}_4^{\mu}) = U_{1,\sin}^{\mu}\sin(2\pi n\bar{x}_4^{\mu}) + U_{1,\cos}^{\mu}\cos(2\pi n\bar{x}_4^{\mu})$ and $\bar{x}_4^{\mu} = q\cdot\bar{x}^{\mu} + t$, with $\bar{x}^{\mu}$ being the coordinate of atom μ in the basic structure.

	$U_{1,\sin}^{x}$	$U_{1,\sin}^{y}$	$U_{1,\sin}^{z}$	$U_{1,\cos}^{x}$	$U_{1,\cos}^{y}$	$U_{1,\cos}^{z}$
Rb1	0.0	0.0	0.016 (2)	0.0	0.0	−0.002 (2)
Rb2	0.0	0.0	−0.012 (2)	0.0	0.0	0.013 (2)
Co	0.0	0.0	−0.009 (2)	0.0	0.0	−0.005 (2)
Br1	0.0	0.0	−0.042 (2)	0.0	0.0	−0.006 (2)
Br2	0.0	0.0	−0.011 (3)	0.0	0.0	−0.062 (2)
Br3	0.008 (4)	0.002 (1)	−0.005 (2)	−0.013 (1)	0.0315 (7)	0.020 (1)

The variations in bond lengths in Rb_2CoBr_4 are in general comparable to those in Rb_2ZnBr_4 (Hogervorst & Helmholdt, 1988; Fig. 4). An exception is the bond length Rb1—Br1^{vii,viii}, which varies in the 0.85 Å range in the Co compound and only 0.31 Å in the Zn-bearing compound.

The bond-valence sums of the cations also show a wide variation when one takes into consideration the modulation (Fig. 5). Here the smallest variation is observed for the Rb1 ion (0.055 v.u.), while the values for Co and Rb2 are considerably larger (Co: 0.2 v.u.; Rb2: 0.18 v.u.).

It has been pointed out before (Fábry & Pérez-Mato, 1994) that the shortest $A^{[11]}$—Br bond plays an important role in the prediction of the stability of an A_2BX_4 compound in the *Pnam* phase. If the ratio of the bond-valence contribution for this contact (designated as *C*1) to the total bond-valence sum reaching the $A^{[11]}$ cation, b.v.(*C*1)/$\sum$b.v.(*C*11), is greater than 0.24, the compound is likely to undergo phase transitions at lower temperatures.

It is remarkable that this bond distance shows no significant variation at all in the modulated phases of Rb_2CoBr_4 and in the isomorphous Rb_2ZnBr_4. The connection of this rigid-body-like behaviour with the observed IC instabilities in A_2BX_4 compounds will be further investigated.

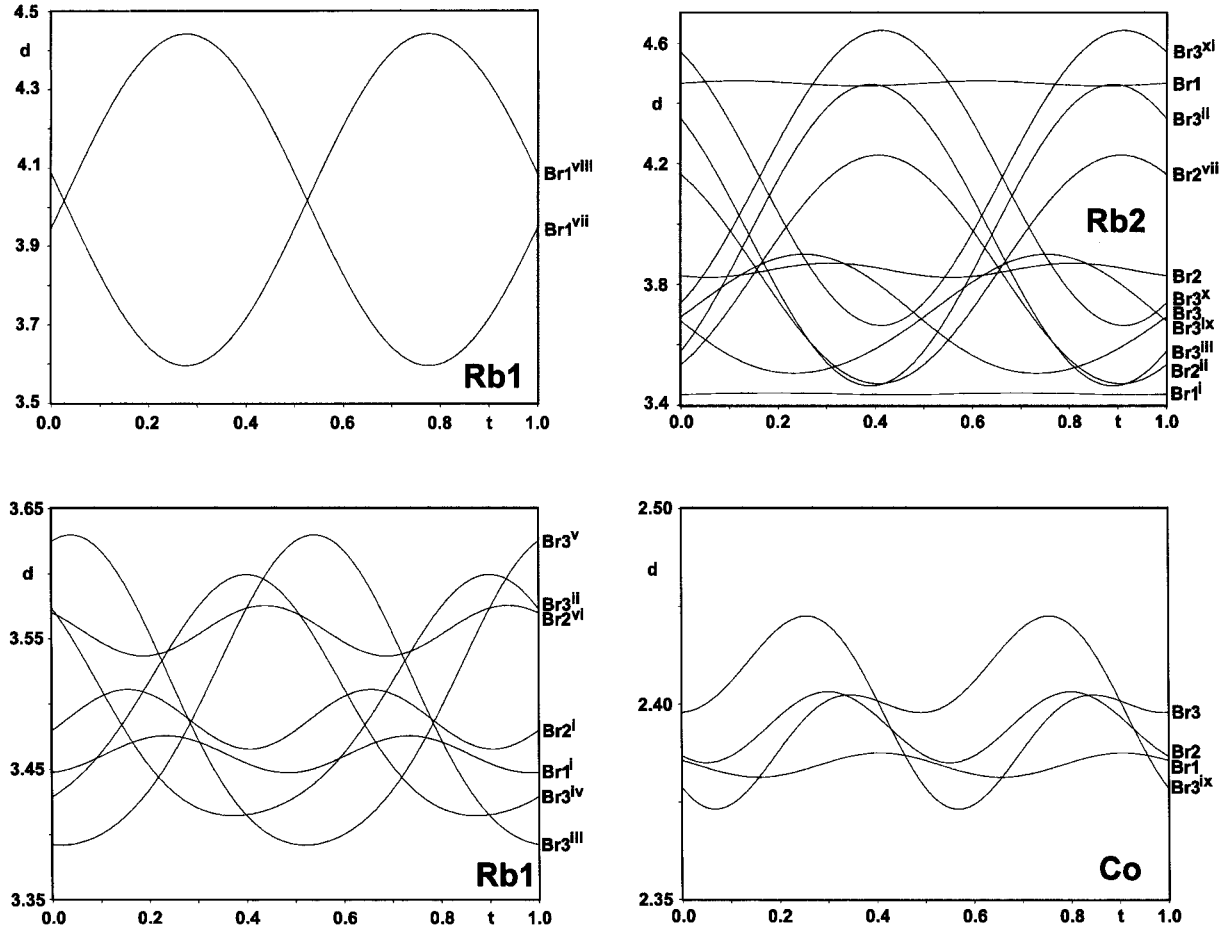

Figure 3
Characteristic interatomic distances in Å as a function of the intrinsic phase *t*. The modulation function is defined as $U_j^{\mu}(\bar{x}_4^{\mu}) = \Sigma_{j=0}^{1}U_{j,s}^{\mu}\sin(2\pi n\bar{x}_4^{\mu}) + U_{j,c}^{\mu}\cos(2\pi n\bar{x}_4^{\mu})$ and $\bar{x}_4 = q\cdot\bar{x}^{\mu} + t$ with $\bar{x}^{\mu}$ being the coordinate of atom μ in the basic structure.

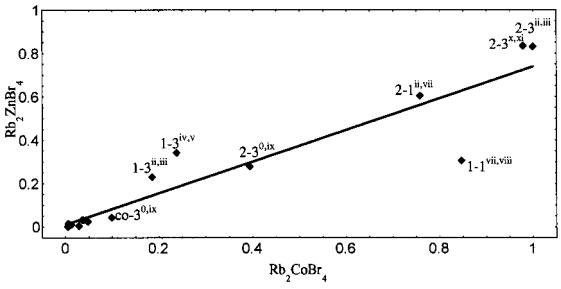

Figure 4
Variation of the bond distances in the incommensurately modulated phases of Rb_2CoBr_4 *versus* Rb_2ZnBr_4 (in Å); first number designates the cation, the second the anion.

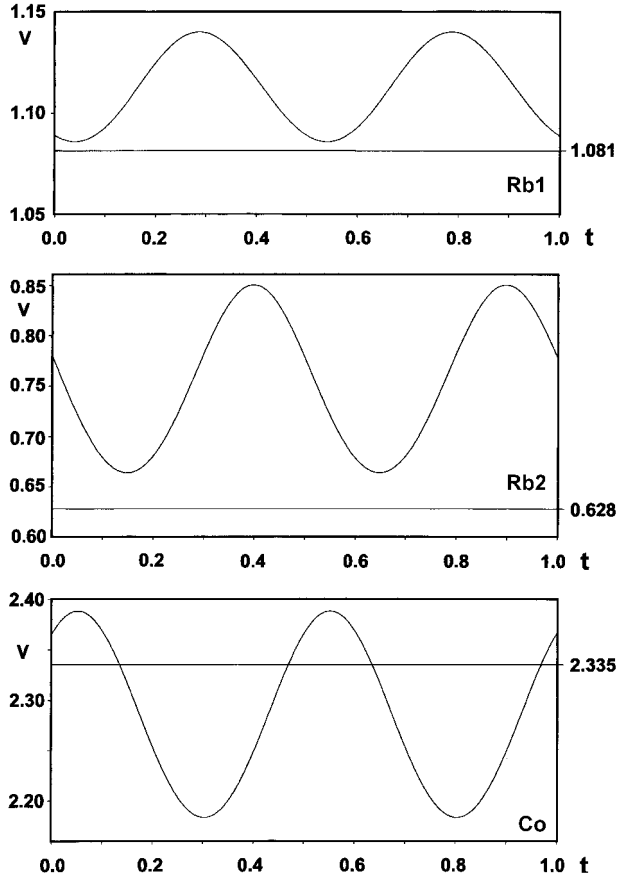

Figure 5
Bond-valence sums *v* for the cations in the incommensurately modulated phase of Rb_2CoBr_4 at 200 K as a function of the intrinsic phase *t*. Bond valences resulting from the average structure at 295 K are given as lines (in [v.u.]).

The authors gratefully acknowledge financial support by the European Union (TMR-Project ERBFMBLCT96-1527), the Gobierno Vasco (PI97/71) and the UPV (EB098/97).

Table 4
Selected bond distances (Å) and angles (°) of the average structure of Rb_2CoBr_4 at room temperature, and minimum and maximum distance in the modulated structure.

In the last column the variation of the distances is given.

	(Å)	Minimum (Å)	Maximum (Å)	Δ (Å)
Rb1—Br2^{i}	3.465 (6)	3.466	3.511	0.045
Rb1—Br1^{i}	3.485 (6)	3.447	3.476	0.029
Rb1—Br3^{ii,iii}	3.494 (5)	3.414	3.599	0.185
Rb1—Br3^{iv,v}	3.502 (5)	3.392	3.630	0.238
Rb1—Br2^{vi}	3.526 (6)	3.537	3.576	0.039
Rb1—Br1^{vii,viii}	4.029 (2)	3.595	4.442	0.847
Rb2—Br1^{i}	3.436 (5)	3.435	3.441	0.006
Rb2—Br3^{0,ix}	3.694 (5)	3.506	3.900	0.394
Rb2—Br2^{ii,vii}	3.861 (6)	3.471	4.229	0.758
Rb2—Br2	3.891 (2)	3.823	3.871	0.048
Rb2—Br3^{ii,iii}	3.941 (7)	3.464	4.464	1.000
Rb2—Br3^{x,xi}	4.196 (7)	3.664	4.643	0.979
Rb2—Br1	4.470 (5)	4.459	4.476	0.017
Co—Br3^{0,ix}	2.378 (4)	2.346	2.445	0.099
Co—Br1	2.380 (6)	2.363	2.375	0.012
Co—Br2	2.381 (6)	2.370	2.388	0.018

Symmetry codes: (0) x, y, z; (i) $-1+x, y, z\#t-1, 0, 0$; (ii) $1-x, 1-y, 1-z\#s-1t1, 1, 1$; (iii) $1-x, 1-y, -\frac{1}{2}+z\#s-3t1, 1, -1$; (iv) $\frac{1}{2}-x, \frac{1}{2}+y, 1-z\#s-2t0, 0, 1$; (v) $\frac{1}{2}-x, \frac{1}{2}+y, -\frac{1}{2}+z\#s-4t0, 0, -1$; (vi) $\frac{1}{2}-x, \frac{3}{2}-y, z\#s2t-1, 1, 0$; (vii) $1-x, 1-y, -z\#s-1t1, 1, 0$; (viii) $1-x, 1-y, 1-z\#s-1t1, 1, 1$; (ix) $x, y, \frac{1}{2}-z\#s3$; (x) $-\frac{1}{2}+x, 1-y, z\#s2t-1, 0, 0$; (xi) $-\frac{1}{2}+x, \frac{1}{2}-y, \frac{1}{2}-z\#s4t-1, 0, 0$.

References

Fábry, J. & Pérez-Mato, J. M. (1994). *Phase Transit.* **49**, 193–229.
Farrugia, L. J. (1996). *ORTEP*3 *for Windows*. University of Glasgow, Scotland.
Friese, K., Madariaga, G. & Breczewski, T. (1998). *Z. Kristallogr.* **213**, 591–595.
Friese, K., Neubert, B., Madariaga, G. & Breczewski, T. (1999). *Z. Kristallogr.* **214**, 1–7.
Gesi, K. (1985). *J. Phys. Soc. Jpn*, **54**, 2401–2403.
Hogervorst, A. C. R. & Helmholdt, R. B. (1988). *Acta Cryst.* B**44**, 120–128.
Kasano, H., Mashiyama, H., Gesi, K. & Hasebe, K. (1987). *J. Phys. Soc. Jpn*, **56**, 831–832.
Pérez-Mato, J. M., Gaztelua, F., Madariaga, G. & Tello, M. J. (1986). *J. Phys. C*, **19**, 1923–1935.
Pérez-Mato, J. M., Zúniga, F. J. & Madariaga, G. (1989). *Phase Transit.* **16/17**, 439–444.
Petříček, V. & Dušek, M. (1998). *JANA*98. Institute of Physics, Academy of the Czech Republic, Praha.
Sawada, S., Shiroishi, Y. & Yamamoto, A. (1978). *Ferroelectrics*, **12**, 413–414.
Seifert, H. J. & Al-Khudair, I. (1975). *J. Inorg. Nucl. Chem.* **37**, 1625–1628.
Sheldrick, G. (1993). *SHELXL. Program for the Refinement of Crystal Structures*. University of Karlsruhe, Germany.
Stoe & Cie (1998*a*). *Stoe IPDS Software*, Version 2.87. Stoe & Cie GmbH, Darmstadt, Germany.
Stoe & Cie (1998*b*). *XRED*. Stoe & Cie GmbH, Darmstadt, Germany.
Yamaguchi, T., Suzuki, H., Shimuzu, F. & Sawada, S. (1987). *J. Phys. Soc. Jpn*, **56**, 4259–4260.